


RESEARCH ARTICLE

The distal arthrogryposis-linked p.R63C variant promotes the stability and nuclear accumulation of TNNT3

Jinfang Lu¹ | Huanzheng Li² | He Zhang³ | Zhengxiu Lin⁴ | Chenyang Xu² |
Xueqin Xu² | Lin Hu⁵ | Zhaotang Luan⁵ | Yongliang Lou¹ | Shaohua Tang^{2,5} 

¹Wenzhou Key Laboratory of Sanitary Microbiology, Key Laboratory of Laboratory Medicine, Ministry of Education, China, School of Laboratory Medicine and Life Sciences, Wenzhou Medical University, Wenzhou, China

²Key Laboratory of Birth Defects, Department of Genetics, Wenzhou Central Hospital, Wenzhou, China

³Zhejiang Provincial Key Laboratory for Subtropical Water Environment and Marine Biological Resources Protection, College of Life and Environmental Sciences, Wenzhou University, Wenzhou, China

⁴The Second Affiliated Hospital and Yuying Children's Hospital of WMU, School of the Second Clinical Medical Sciences, Wenzhou Medical University, Wenzhou, China

⁵Key Laboratory of Medical Genetic, School of Laboratory Medicine and Life Science, Wenzhou Medical University, Wenzhou, China

Correspondence

Shaohua Tang, Center of Prenatal Diagnosis, Wenzhou Central Hospital, Dajianxiang 32, Wenzhou, China.
Email: tsh006@126.com

Funding information

start-up funding from Wenzhou Medical University, Grant/Award Number: QTJ19019; Wenzhou Scientific Bureau, Grant/Award Number: Y20170020; Medical Scientific Projects from Health Bureau of Zhejiang Province, Grant/Award Number: 2019RC275; Zhejiang Provincial Natural Science Foundation of China, Grant/Award Number: Q16H200001; National Key Research and Development Plan of China, Grant/Award Number: 2018YFC1002702

Abstract

Background: Distal arthrogryposis (DA) is comprised of a group of rare developmental disorders in muscle, characterized by multiple congenital contractures of the distal limbs. Fast skeletal muscle troponin-T (TNNT3) protein is abundantly expressed in skeletal muscle and plays an important role in DA. Missense variants in *TNNT3* are associated with DA, but few studies have fully clarified its pathogenic role.

Methods: Sanger sequencing was performed in three generation of a Chinese family with DA. To determine how the p.R63C variant contributed to DA, we identified a variant in *TNNT3* (NM_006757.4): c.187C>T (p.R63C). And then we investigated the effects of the arginine to cysteine substitution on the distribution pattern and the half-life of TNNT3 protein.

Results: The protein levels of TNNT3 in affected family members were 0.8-fold higher than that without the disorder. TNNT3 protein could be degraded by the ubiquitin-proteasome complex, and the p.R63C variant did not change TNNT3 nuclear localization, but significantly prolonged its half-life from 2.5 to 7 h, to promote its accumulation in the nucleus.

Conclusion: The p.R63C variant increased the stability of TNNT3 and promoted nuclear accumulation, which suggested its role in DA.

KEYWORDS

distal arthrogryposis, nuclear accumulation, protein stability, skeletal muscle, TNNT3

Jinfang Lu and Huanzheng Li equally contributed to this work.

This is an open access article under the terms of the Creative Commons Attribution-NonCommercial-NoDerivs License, which permits use and distribution in any medium, provided the original work is properly cited, the use is non-commercial and no modifications or adaptations are made.

© 2021 The Authors. *Journal of Clinical Laboratory Analysis* published by Wiley Periodicals LLC.

1 | INTRODUCTION

Distal arthrogryposis is a group of autosomal dominant muscle disorders characterized by non-progressive congenital contracture of the distal limb. It is a common birth defect and occurs in one in 3000–5000 new births.^{1,2} DA can be clinically classified into 10 types (DA1–DA10) with several overlapping features, although each specific type is relatively rare.^{1,3} To date, several genes have been reported to be linked with DA, such as β -tropomyosin (*TPM2*, OMIM 190990),^{3,4} myosin-binding protein C1 (*MYBPC1*, OMIM 160794),⁵ myosin heavy chain 3 (*MYH3*, OMIM 160720),^{6,7} troponin I type 2 (*TNNI2*, OMIM 191043),^{2,8} fast skeletal muscle *TNNT* (*TNNT3*, OMIM 600692),^{2,9–12} and others.^{2,13} *TPM2* stabilizes actin filaments and mediates the interaction between actin and the troponin complex.^{3,4} *MYBPC1* is abundantly expressed in slow skeletal muscle and interacts with the sarcomeric myosin, actin, and creatine kinase.⁵ *MYH3* is an ATP-dependent motor protein that drives muscle contraction.^{6,7} *TNNI2* and *TNNT3* are vital components of the troponin complex and play an important role in the regulation of muscle contraction and relaxation.^{14,15} Mutations in these contractile-related genes are the genetic basis for approximately 50% of all DA patients.^{2,13} However, few studies have reported possible molecular mechanisms responsible for this disorder.

In vertebrates, *TNNT* family members expressed in striated muscle include three homologous variants: slow skeletal muscle *TNNT* (*TNNT1*, GenBank: NC_000019.10); cardiac muscle *TNNT* (*TNNT2*, GenBank: NC_000001.11); and *TNNT3* (GenBank: NC_000011.10).^{15,16} The isoform proteins share highly conserved middle and carboxyl-terminal regions. Although the amino acids in the N-terminal region are significantly hypervariable, they can also modulate the conformation and function of the *TNNT* core structure to fine-tune muscle contractility.^{15,17} *TNNTs* can interact with the Ca^{2+} -binding subunit troponin C and the inhibitory subunit troponin I to form heterotrimeric complex.^{10,14,15} Additionally, *TNNTs* consist of an excitation-contraction complex and can anchor troponin complex to tropomyosin. The troponin complex regulates excitation-contraction coupling and contraction of striated muscle to generate force.^{10,14,15}

Mutations of *TNNT* members are associated with numerous muscle diseases. Loss of human *TNNT1* (OMIM 191041)¹⁸ or *TNNT2* (OMIM 191045)¹⁹ can cause severe nemaline myopathies, and approximately 10 DA kindreds with *TNNT3* variants had been reported in different countries.^{2,9,11,12} Some pathogenic variants, such as p.R63H, p.R63C, and p.R63S, have been identified in patients from different countries with DA1 (OMIM 108120, <http://www.omim.org>) or DA2B (OMIM 601680, <http://www.omim.org>).^{2,9,11,12} Their DA phenotypes follow an autosomal dominant inheritance pattern, but the boundaries between the different subtypes are indistinct under some conditions.^{2,9,11,12} Residue 63rd of *TNNT3* is a hot mutated point and almost all reported deleterious variants are associated with this residue.^{2,9,11,12} Recently, two splicing variants with a frameshift in *TNNT3* were reported responsible for a specific, recessively inherited subtype of nemaline myopathy and DA.^{20,21}

The normal pathogenic roles of *TNNT3* variants involve functional disruption of the troponin complex.¹⁰ For example, the *TNNT3*-p.R63C variant might cause limb defects by significantly enhancing ATPase activity to interfere its interaction with tropomyosin and to produce hypercontractile muscles *in vivo*.¹⁰ Furthermore, *TNNT3* and other troponin subunits (i.e., cardiac troponin C, troponin T, and troponin I) have recently been found in the nuclei of different cells, such as cervical carcinoma (HeLa), epidermoid carcinoma (A-431), and osteosarcoma cells (U-2 OS).^{22,23} Growing evidence has suggested that *TNNT3* could serve as a transcriptional regulator and overexpression of *TNNT3* induces apoptosis.^{22–25} Chromatin immunoprecipitation sequencing analysis has also shown that the binding motif of *TNNT3* overlapped with that of P53.²⁶ These results challenge the conventional view of troponin as a sarcomere-specific protein that is exclusively involved in muscle contraction.^{22,23,25} However, the molecular mechanism of DA caused by the *TNNT3* variant is still not fully understood.

In the present study, we identified and characterized a *TNNT3* (NM_006757.4): c.187C > T (p.R63C) variant in a Chinese family with typical DA2B syndrome. We experimentally investigated the consequences of replacing arginine with cysteine. Our results showed that *TNNT3* was aberrantly expressed in affected patients and was 0.8-fold higher than that of age-matched controls. The *TNNT3*-p.R63C variant was mainly localized in the nucleus, where it formed sharp puncta in foci with different subnuclear distribute pattern. *TNNT3*-p.R63C significantly accumulated in nuclei and its half-life was prolonged. Together, the results suggested that the non-canonical function of *TNNT3* might play an important role in the pathogenesis of DA.

2 | MATERIALS AND METHODS

2.1 | Materials

HEK293 cells were obtained from the American Type Culture Collection (Manassas, VA, USA). Dulbecco's Modified Eagle Medium (DMEM) (# 12430-047), fetal bovine serum (FBS) (# 16000-044), 0.05% trypsin/EDTA (# 25300-054), Opti-MEM media (# 31985-070), TRIzol reagent (# 10296010), 4',6-diamidino-2-phenylindole (DAPI, P36931), Lipofectamine 2000 (# 11668-019), Power SYBR[®] Green PCR Master Mixture (# 2011605), and enhanced chemiluminescence substrate (# 34094) were all from Thermo Fisher Scientific (Waltham, MA, USA). Protease-inhibitor cocktail (# p8340) and cycloheximide (# C7698) were from Sigma-Aldrich (St. Louis, MO, USA). PrimeScript[™] RT reagent kit with gDNA Eraser (# RR047A), pMD[™]18-T Vector Cloning Kit (# 6011), ligation kit (# 6022), PrimeSTAR[®] HS DNA Polymerase (# R010A), and restriction enzymes were from Takara Bio (Dalian, China). Phenylmethanesulfonyl fluoride (PMSF, # ST505), protease inhibitor cocktail for mammalian cell and tissue extracts (# P1010), penicillin-streptomycin (# C0222), BCA Protein Assay Kit (# P0012), and QuickMutation[™] Site-Directed

Mutagenesis Kit (# D0206) were all from Beyotime Biotechnology (Shanghai, China). MG-132 (# S2619) was from Selleck (Shanghai, China). Primary antibodies anti-Myc (# 2272), anti-glyceraldehyde 3-phosphate dehydrogenase (GAPDH, # 5174), anti- β -tubulin (# 2146), anti- β -actin (# 3700), and monoclonal anti-H3 (# 14269) were from Cell Signaling Technology (Danvers, MA, USA). Rabbit polyclonal antibody to TNNT3 (# ab175058) was from Abcam (Cambridge, MA, USA), and horseradish peroxidase-conjugated secondary antibodies were from Millipore (St. Louis, MO, USA).

2.2 | Sanger sequencing

Potential variants of the *TNNT3* gene in patient family members and 10 healthy controls were identified by Sanger sequencing. The genomic DNA was isolated from peripheral blood or amniocytes using a Qiagen DNA Blood Mini Kit (#51104, Qiagen, Hilden, Germany) according to the manufacturer's instructions. Specific primers (listed in Table S1) were designed to amplify sequences containing previously reported mutation sites of *TNNT3*.² DNA fragments were amplified using polymerase chain reaction (PCR). The 50- μ l PCR reaction mixture contained 50-ng genomic DNA, 1- μ l PrimeSTAR[®] HS DNA polymerase (Takara Bio), 1- μ l forward primer, and 1- μ l reverse primer. PCR reactions were performed as follows: 95°C for 5 min, 30 cycles (95°C for 30 s, 55°C for 30 s, and 72°C for 40 s); 72°C for 10 min; and 4°C for 15 min. PCR products were purified and then sequenced by an ABI 3100 automated DNA sequencer (Applied Biosystems, CA, USA). Sequencing results were aligned to the human genome reference (<http://www.ensembl.org/>), and nucleotide changes were identified according to their position in the wild-type *TNNT3* reference sequence. This study was approved by the Ethics Committee of Wenzhou Central Hospital, and written informed consent was obtained from the participants.

2.3 | Plasmid constructs

Total RNA from human skeletal muscle (previously collected from aborted fetuses affected with embryo arrest and stored at -80°C in our laboratory) and the reverse transcription reaction were used to generate cDNA by the PrimeScript[™] RT reagent kit with gDNA Eraser. PCR amplification was conducted with the corresponding primers (listed in Table S1). The fragments containing the entire coding sequence of human *TNNT3* were cloned into the appropriate sites (EcoRI/HindIII or HindIII/KpnI) of the pcDNA3.1-Myc (Invitrogen, Carlsbad, CA, USA) and pEGFP-N1 vector (Clontech, San Jose, CA, USA) to create pcDNA3.1/*TNNT3*-Myc and pEGFP-N1/*TNNT3* (translational fusion with a green fluorescence protein encoding gene), respectively. The variant c.187C > T (p.R63C) was introduced to *TNNT3* cDNA by Site-Directed Mutagenesis Kit following the manufacturer's instructions. The pcDNA3.1/*TNNT3*-Myc or pEGFP-N1/*TNNT3* was used as a template. After confirming the sequences, they were designated as pcDNA3.1/*TNNT3*, pcDNA3.1/*TNNT3*-mut,

pEGFP-N1/*TNNT3*, and pEGFP-N1/*TNNT3*-mut. Plasmids were purified by using a Plasmid Midi Kit (Qiagen).

2.4 | Cell culture and transfection

Cells were cultured in DMEM containing 10% FBS, 100 U/ml penicillin, and 100 μ g/ml streptomycin. The cultures were maintained in a humidified 5% CO₂ incubator at 37°C, and cells were passaged using 0.05% trypsin/EDTA. Two microgram of plasmid (pcDNA3.1, pcDNA3.1/*TNNT3* or pcDNA3.1/*TNNT3*-mut) was transfected into cells cultured in 6-well plates (4 \times 10⁵ cells/well), and the Lipofectamine 2000 reagent was used for cell transfection according to the manufacturer's instructions. After transfection, the transfected cells were incubated at 37°C for additional 48 h for western blotting. To determine the subcellular localization of TNNT3 and TNNT3-p.R63C, cells (8 \times 10⁴ cells/well) were cultured on coverslips in 12-well plates, and then 0.5 μ g of plasmid (pEGFP-N1, pEGFP-N1/*TNNT3*, or pEGFP-N1/*TNNT3*-mut) was transfected, and the plates were incubated for 48 h at 37°C. The cells were fixed with formaldehyde (4%) for 30 min, washed twice with 1 \times phosphate-buffered saline (PBS). DAPI was added and incubated at room temperature for 20 min for nuclear staining according to the manufacturer's instructions. Images were captured with a fluorescence microscope (DMi8; LEICA, Wetzlar, Germany), and the localization was assessed.

2.5 | Western blotting

Cells were transfected with plasmids (pcDNA3.1-Myc, pcDNA3.1/*TNNT3*, or pcDNA3.1/*TNNT3*-mut). After 48 h, the cells were harvested, lysed, and immunoblotted in accordance with standard protocols. Briefly, cells were washed once with PBS and then lysed in a radioimmunoprecipitation assay buffer supplemented with PMSF and protease-inhibitor cocktail. The cell lysates were collected, and protein concentrations were determined using the BCA Protein Assay Kit. Each lane was loaded with 40 μ g of sample (whole cell lysis) and then fractionated using a 12% sodium dodecyl sulphate-polyacrylamide gel electrophoresis gel, followed by transfer to a polyvinylidene difluoride membrane (GE Healthcare Life Sciences, Marlborough, MA, USA) using a Trans Blot apparatus (Bio-Rad, Hercules, CA). The membranes were blocked with 5% non-fat milk in PBS for 1 h at room temperature and then probed with the appropriate primary antibodies overnight at 4°C. Then, the corresponding peroxidase-conjugated secondary antibodies (1:5000) were used, respectively. The targeted proteins were visualized by using enhanced chemiluminescence reagents with a ChemiDoc[™] MP Imaging System (Bio-Rad). Western blotting data were quantified by ImageJ software (National Institutes of Health, Bethesda, MD, USA). The intensity of each band was divided by the intensity of its respective loading control to provide normalized values used for statistical analysis.

2.6 | Cell fractionation

Cells were fractionated using the Nuclear and Cytoplasmic Protein Extraction Kit (Beyotime Biotechnology, Shanghai, China) according to the manufacturer's instructions. Briefly, HEK293 cells were seeded at the desired densities in six well plates and incubated at 37°C, with 5% CO₂ for 24 h. Forty-eight hours after transfection, the cells were collected and resuspended in ice-cold hypotonic lysis buffer with 1 mM PMSF, homogenized, and centrifuged (4°C, 5 min at 13 000 g) to collect the supernatant containing cytoplasmic proteins. Then, 100- μ l nuclear extraction buffer was added to resuspend the pellet, followed by vortex and incubation on ice for 30 min. Further centrifugation at 13 000 g at 4°C for 10 min was performed to collect the supernatant, which contained nuclear proteins. Finally, 200 μ l of the cytoplasmic fraction and 50 μ l of the nuclear fraction were obtained for each sample. Protein content of each fraction was measured and analyzed by western blotting.

2.7 | Quantitative PCR

HEK293 cells were transfected with the pEGFP-N1, pEGFP-N1/*TNNT3*, and pEGFP-N1/*TNNT3*-p.R63C vectors. After 48 h, total RNA was isolated from with TRIzol reagent following the manufacturer's instructions. Elimination of genomic DNA and cDNA synthesis were performed using PrimeScript™ RT reagent kit with gDNA Eraser as previously described.²⁷ Gene specific primers for *TNNT3* and *GAPDH* were designed (listed in Table S1). The quantitative PCR reactions followed the manufacturer's instructions. The qRT-PCR reaction mixture had a final volume of 20 μ l, containing 2- μ l diluted cDNA template, 7 μ l of nuclease free water, 0.5 μ l of each gene-specific primer (10 pmol/ μ l), and 10 μ l of the Power SYBR® Green PCR Master Mixture (Thermo Fisher Scientific). All PCR reactions occurred in a 96-well ABI plate format in ViiA7 (Life Technology, NY, USA). For quantitative PCR, the cycling conditions was initiated at 50°C for 2 min, with a secondary step at 95°C for 10 min, followed by 40 cycles of PCR reactions (95°C for 10 s and 58°C for 1 min). The reaction specificity was examined using dissociative curves. The *TNNT3* relative mRNA expression levels were obtained by normalization to *GAPDH* using the 2^{- $\Delta\Delta$ Ct} method. All qRT-PCR data were obtained in triplicate.

2.8 | Statistics

All experiments were performed in triplicate, and the results expressed as the mean \pm standard deviation. The data were analyzed by Prism 8 (GraphPad, La Jolla, CA, USA). Student's *t* test was used to determine the difference between two groups. One-way analysis of variance with Tukey's multiple comparison test was used to evaluate

significant differences between multiple groups. The *p* values are indicated on each figure as <0.05 (*), <0.01 (**), and <0.001 (***)

3 | RESULTS

3.1 | Clinical manifestation and identification of the disease-causing variant

A patient (the proband) with typical DA features and her family members were enrolled at the Department of Clinical Laboratory, Wenzhou Central Hospital/Dingli Clinical School of Wenzhou Medical University. Using clinical follow-up observations, we found this family contained five affected members over three generations (including two aborted fetuses) (Figure 1). All live patients had normal cognitive levels. Their detailed clinical data were evaluated by at least two senior neurologists and surgeons from our hospital.

The proband (III:1) was a 7-year-old female who had bilateral and congenital contractures of the distal limbs. Her hands showed severe camptodactyly, adducted thumbs, mild cutaneous syndactyly of the second to fifth fingers, and ulnar deviation of fingers. Both the grandfather (I:2) and father (II:2) of the proband showed hand deformities similar to the proband (Figure 1B and D), while their feet were normal. The proband's mother had been pregnant four times, and the proband was the first and only live baby. III:3 and III:4 were aborted because of severe arthrogryposis of the distal limbs revealed by ultrasound images during prenatal diagnosis in our hospital, and III:2 was naturally aborted because of unknown reasons (Figure 1A). Detailed clinical information and X-ray images of the hands are available (Figure 1B–G and Table 1). Based on the clinical manifestations and the autosomal dominant inheritance pattern, this family was diagnosed as putative DA (Figure 1).

To identify the sequence variant associated with DA, blood samples were obtained from three affected individuals (I:2, II:2, and III:1) and healthy family members (II:1, II:3, and III:2). Sanger sequencing was conducted to analyze DA-associated genes, which have been previously reported and identified a heterozygous missense mutation c.187C > T in exon 9 of the *TNNT3* gene (Figure 1H–J). The variant was not detected in unaffected family members (Figure 3K). This variant resulted in an arginine-to-cysteine substitution at residue 63 (p.R63C) of I:2, II:2, and III:1 (Figure 1H–J). R63 is a conserved position in some vertebrates (Figure 1N). Variants in this site had been reported to be associated with DA in China and other countries and have been predicted to have deleterious effects.^{9,11,12} However, the mechanism underlying these effects is not fully understood.

3.2 | The p.R63C point mutation increased *TNNT3* protein stability

To assess the specific consequence of the p.R63C variant on *TNNT3*, we performed western blotting analysis, which showed an increase

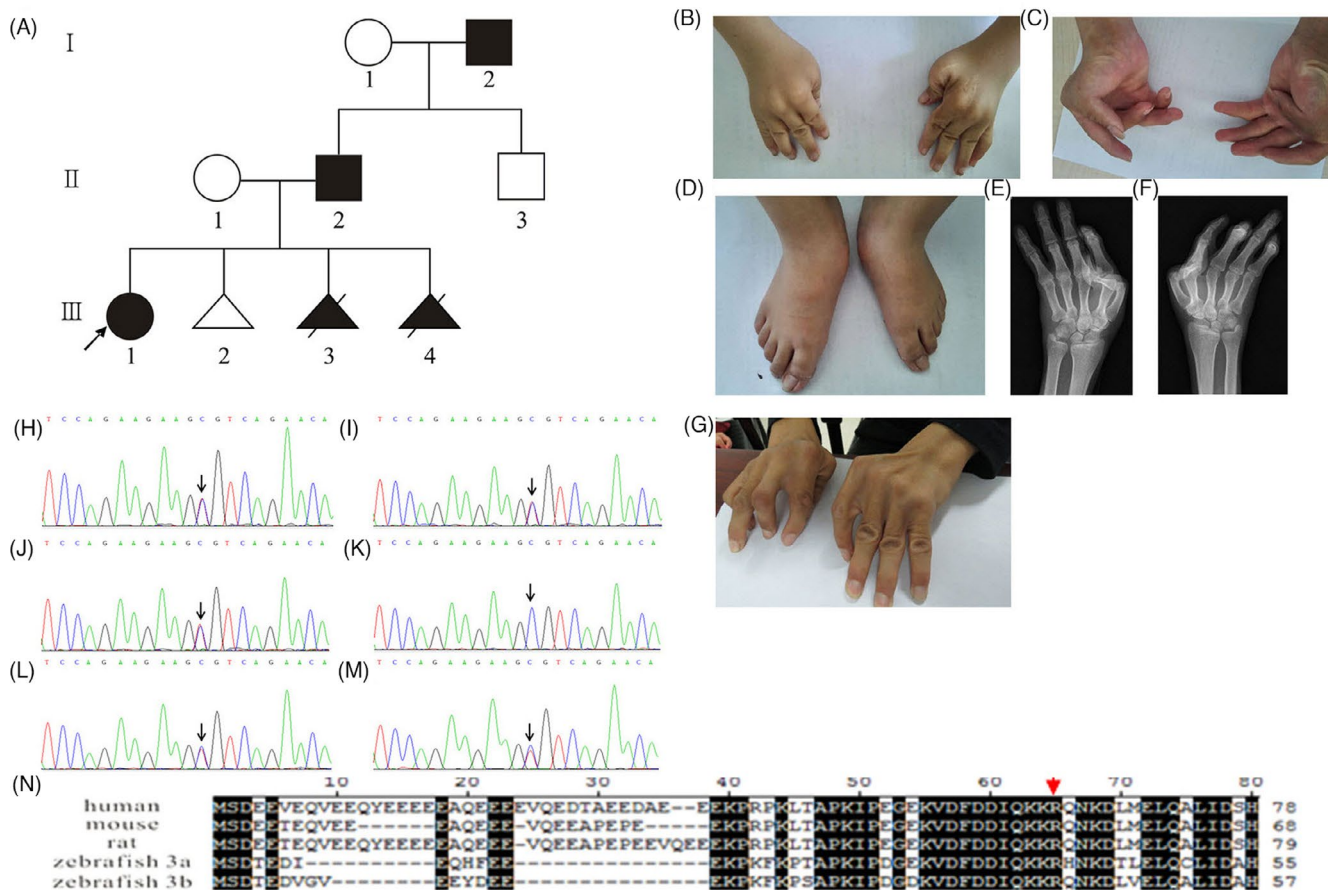


FIGURE 1 Identification of the *TNNT3* variant in affected family members with DA. (A) The pedigree of the family members affected by DA. Squares and circles represent males and females, respectively. Triangles symbolize an aborted fetus. The clinically affected individuals are indicated by filled symbols. The arrows beside the circle represent the proband. (B) and (D) Hand and foot images of the proband. The hand image (C) and its X-ray images (E and F) of the proband's father. (G) The hand photographs of the proband's grandfather. The scripts in Figure 1H–J indicate sequencing results of the proband, I:2 and II:2, whereas the script in (K) indicates sequencing results of a healthy member of the affected family. The scripts in (L) and (M) indicate the sequencing results of amniotic fluid cultures for III:3 and III:4. (N) Protein sequences of *TNNT3* from human, mouse, rat, and zebrafish were aligned to indicate a conserved Arg at residue 63 in *TNNT3*

of total *TNNT3* protein in the skeletal muscle of affected subjects, when compared to unaffected subjects (Figure 2A). The level of *TNNT3* in DA samples was approximately 0.8-fold higher than that of unaffected subjects (Figure 2B, $p = 0.001$), so we speculated that there was a relationship between the p.R63C variant and the *TNNT3* protein levels. Plasmids expressing wild-type or the p.R63C variant *TNNT3* were therefore transfected into HEK293 cells, and protein levels were detected at indicated times. The *TNNT3*-p.R63C protein level was approximately 2.6-fold higher than *TNNT3* at 24 h after transfection (Figure 2C and D, $p = 0.001$). While at 48 h, it was still 1.7-fold higher than that of the wild type (Figure 2D, $p = 0.000$). The difference of protein levels might have been caused by different transcription levels in each group. However, qRT-PCR analysis showed that there was no significant difference in mRNA level between the wild-type and the *TNNT3*-p.R63C variant (Figure S1). The results therefore ruled out the possibility that the difference of protein levels was due to different transcription levels. Thus, we speculated that the increase of *TNNT3*-p.R63C protein was due to its higher stability.

We then measured the half-life of *TNNT3* and its variant by cycloheximide (CHX) chase analysis. Forty-eight hours after transfection, 50 $\mu\text{g/ml}$ CHX was added to the medium, and cells were harvested at the indicated times. Figure 3 showed that the half-lives of *TNNT3* and *TNNT3*-p.R63C were estimated to be approximately 2.5 and 7 h, respectively. This result suggested that wild-type *TNNT3* was degraded faster than *TNNT3*-p.R63C, a result that was compatible with lower *TNNT3* protein levels in unaffected subjects and in HEK293 cells that were transfected with wild type and variant plasmid (Figure 3).

Due to its short half-life, *TNNT3* might be degraded by the proteasome pathway. To test this possibility, we treated transfected cells with CHX plus the proteasome inhibitor MG132, which increased the residual levels of *TNNT3*-p.R63C and *TNNT3* at all time points, when compared with the CHX treated groups (Figure 4 and S2). However, the half-life of *TNNT3*-p.R63C was still 1-fold higher than that of *TNNT3* (12 h vs 6 h) (Figure 4). Even at 24 h, the residual amount of *TNNT3*-p.R63C was significantly higher than that of *TNNT3*-WT. Therefore, the p.R63C variant enhanced the intrinsic protein stability of *TNNT3* (Figure 4).

	I:2	II:2	III:1	III:3	III:4
Age/sex	60/M	29/M	7/F	Aborted	Aborted
Decreased facial expression	-	-	-	ND	ND
Ear deformity	-	-	+	-	-
Small pursed mouth	-	-	-	ND	ND
Triangularly shaped face	-	-	-	ND	ND
Finger contractures	+	+	+	+	+
Camptodactyly	+	+	+	+	+
Elbow contractures	-	-	+	ND	ND
Limited wrist extension	-	-	+	ND	ND
Asymmetric legs/feet	-	-	+	+	+
Clubfeet	-	-	+	+	+
Scoliosis	-	-	-	ND	ND
Short stature	-	-	-	ND	ND
Surgical operations	-	-	+	-	-
DA classification	DA2B				
Disease-causing mutation	TNNT3:c.187C>T (p.R63C)				

Note: +, present; -, absent; ND, not determined. M, male; F, female.

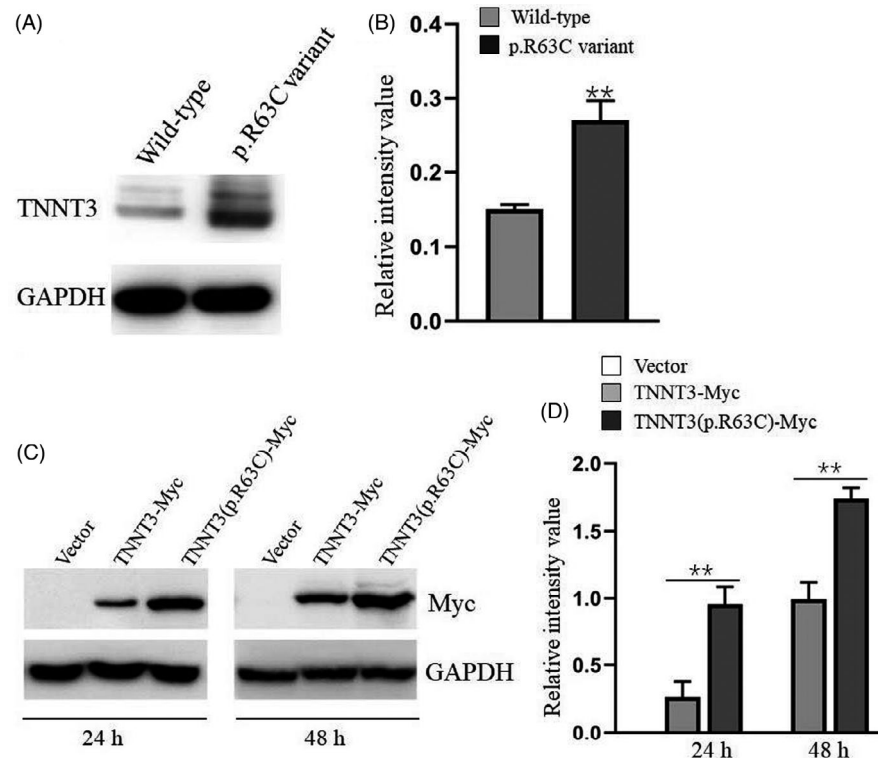


TABLE 1 Clinical phenotypes of affected individuals with *TNNT3* gene mutation in a Chinese family

FIGURE 2 The effect of the p.R63C variant on TNNT3 protein levels. TNNT3 protein levels in skeletal muscles from affected and non-affected members were assessed by western blotting (TNNT3 antibody, 1:500). Representative images are shown in A, and GAPDH (1:5000) was used as an internal loading control. The relative optical density of TNNT3/GAPDH is indicated in B. TNNT3 protein levels were assessed *in vitro* using an anti-Myc antibody (1:500) at different time points after transfection. Representative western blotting images in C and GAPDH (1:5000) were used as internal loading controls. The relative optical density ratio of TNNT3/GAPDH is shown in D. The results are presented as the mean \pm SD, and ** $p < 0.01$ indicates significant differences, when compared with the corresponding wild-type values

3.3 | TNNT3-p.R63C mainly accumulated in the nucleus

Next, we investigated where TNNT3-p.R63C accumulated in cells. Some studies have reported that TNNT3 was translocated into the nucleus,^{24,25} so we speculated that the p.R63C variant might change the distribution pattern of TNNT3 and slow its turnover.

To test our hypothesis, we performed a green fluorescent protein (GFP) subcellular localization assay. *TNNT3* and *TNNT3*-p.R63C variant were translationally fused to GFP, and the subcellular localization was determined using an inverted fluorescence microscopy. GFP expressed by the empty vector showed a diffuse distribution, and fluorescence was observed in the whole cell (Figure 5A). In contrast, the GFP-tagged TNNT3 and p.R63C

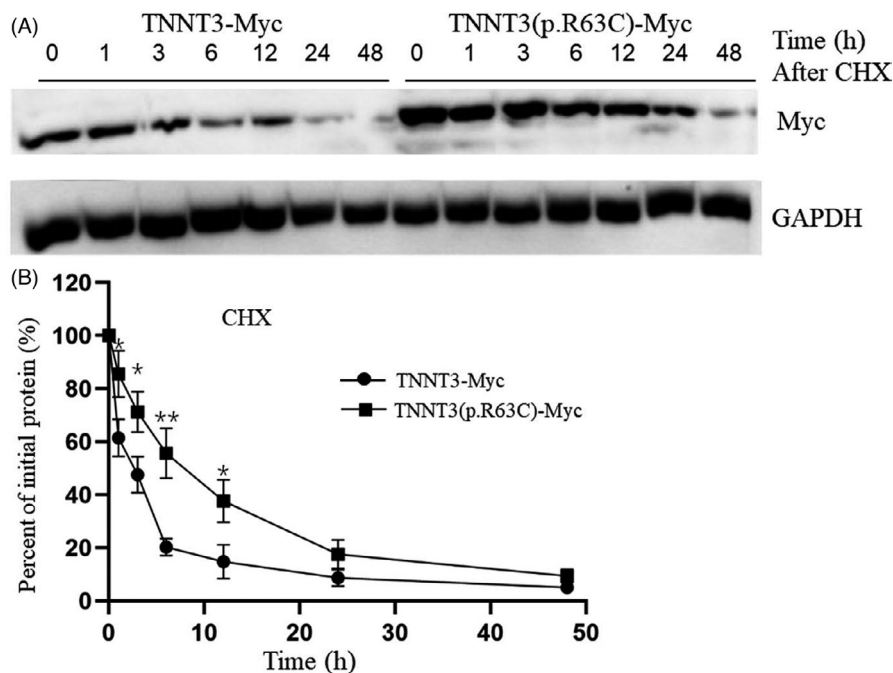


FIGURE 3 The p.R63C variant extended the half-life of TNNT3. HEK293 cells were transfected with *TNNT3* or p.R63C variant constructs, and then the cells were incubated in medium containing cycloheximide (50 μ g/ml) and then chased for the indicated times. The cells were harvested at different time points, and TNNT3 protein levels were determined by western blotting using anti-Myc antibody (1:500). Each lane resolved 40 μ g of protein, and representative western blot images are shown in A. (B) The relative ratios of the optical band densities of TNNT3/GAPDH were normalized as the percentage of the ratios of the starting point as 100%. The results are presented as the mean \pm SD from three independent experiments, and * p < 0.05 and ** p < 0.01 indicate significant differences, when compared to the corresponding values of TNNT3-Myc

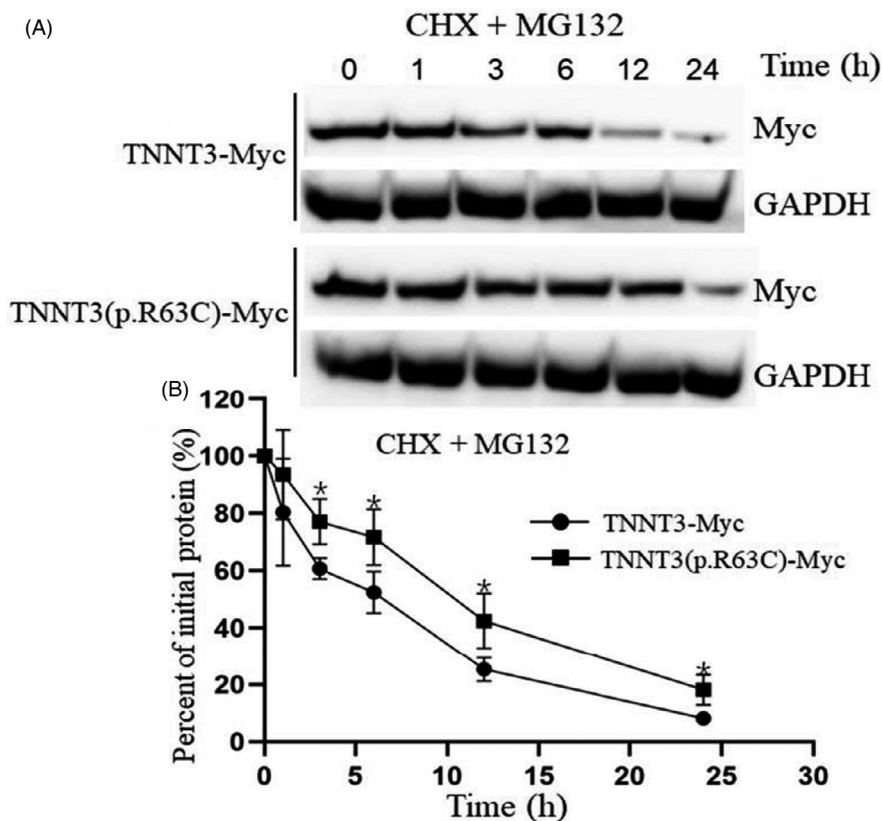


FIGURE 4 The effect of MG132 on the half-lives of TNNT3 and the p.R63C variant. Plasmids encoding *TNNT3* or the p.R63C variant were individually transfected into HEK293 cells and then incubated in medium containing either 0.1% dimethyl sulfoxide or 10 μ M MG132 for 3 h. Cycloheximide (50 μ g/ml) was then added to the cultures, and the cells were harvested at the indicated time points. (A) Representative western blotting images. (B) The protein levels designated by the ratios of TNNT3/GAPDH (solid circle) and TNNT3-p.R63C/GAPDH (solid square) were normalized to the ratios of the starting point without drug treatment. The results are presented as the mean \pm SD from three independent experiments, and * p < 0.05 indicates significant differences, when compared to the corresponding values of TNNT3-Myc

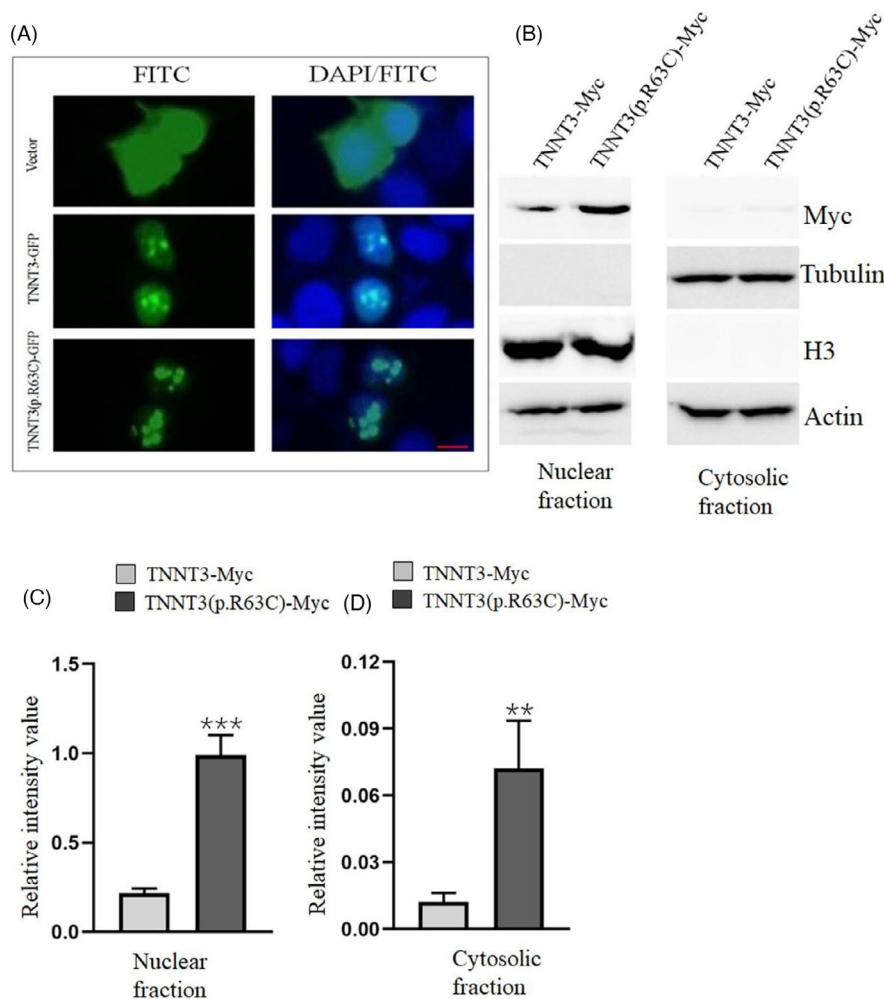


FIGURE 5 The p.R63C variant promoted its nuclear translocation and formed aggregated puncta. (A) The plasmids encoding fusion proteins, TNNT3-EGFP, TNNT3-p.R63C-EGFP, and empty vector, were transfected into HEK293 cells. After 2 days, the cultures were observed using an inverted fluorescent microscope with a GFP filter. The DAPI indicated nuclei with blue fluorescence. Scale bar, 10 μ m. (B) HEK293 cells were transfected with the TNNT3- or p.R63C variant-expressing vectors, and cytosolic and nuclear proteins were separated. TNNT3 protein levels in different fractions were determined with western blotting using anti-Myc antibody (1:500). Anti-actin (1:5000) was used as the internal control. Anti-Histone 3 (1:5000) was used as the loading control for nuclear TNNT3. (C, D) The relative optical densities of TNNT3/actin are indicated. The results are presented as the mean \pm SD from three independent experiments, and ** $p < 0.01$ and *** $p < 0.001$ indicate significant differences, when compared with the corresponding values of TNNT3-Myc

variant were localized in the nucleus and formed distinctive sharp puncta. It is worth noting that there was a considerable amount of TNNT3-GFP distributed in the whole nuclei (Figure 5A). The nuclear localizations of TNNT3 and TNNT3-p.R63C were different from each other as shown by the more aggregation-prone pattern for the former (Figure 5).

To further validate the protein distribution pattern, we fractionated the nuclear and cytoplasmic protein components (Figure 5B). The purity of each fraction was verified by a cytoplasmic marker (α -tubulin) and nuclear marker (Histone H3), respectively. The α -tubulin was predominantly detected in the cytoplasmic fraction, and Histone H3 was only found in the nuclear fraction. Actin was consistently found in both the cytoplasmic and nuclear fractions. Thus, separation of nuclei and cytosol was successful (Figure 5B). Western blotting results showed that both TNNT3 and TNNT3-p.R63C were mainly localized in the nucleus, but the level of TNNT3-p.R63C was approximately 3.5-fold higher than that of TNNT3 (Figure 5B and C), while only a small amount of TNNT3-p.R63C was detected in the cytoplasm, comprising approximately 5% of its total contents (Figure 5B and D). Collectively, the results showed that the p.R63C variant positively contributed to the stability of TNNT3 and promoted its nuclear accumulation.

4 | DISCUSSION

Using prenatal diagnosis, we identified a Chinese family with DA2B, as determined by their affected hands, with an autosomal dominant inherited pattern, and a c.187C > T (p.R63C) variant in *TNNT3*, which was consistent with a previous report.¹¹ The arginine residue at position 63 was located in the highly variable N-terminus of the protein, which has been a region of many mutations. At present, all reported DA-linked amino acid substitutions occurring in *TNNT3* were located at this residue.^{2,9,11,12} Protein alignment analysis also implied that R63 was conserved from humans to zebrafish (Figure 1N). In this regard, regulation of *TNNT3* function by R63 is possibly a common mechanism in many species. However, identification of the pathogenic role involving the p.R63C variant is still unknown, which was the objective of this project.

When assessing *TNNT3* protein levels in clinical muscle samples, we found an unexpected 45% reduction in age-matched controls, when compared with DA patients. When the same amount of *TNNT3* or *TNNT3*-p.R63C expressing plasmid was transfected into HEK293 cells lacking endogenous *TNNT3*, western blotting results showed that the *TNNT3* protein was approximately 43–73% less than that of the *TNNT3*-p.R63C variant (Figure 2), although their

transcription levels were similar (Figure S1). The difference of protein levels may have resulted from their intrinsic protein stabilities. Chase experiments were therefore conducted to show that the half-life of TNNT3-p.R63C was approximately 1.8-fold higher than that of TNNT3 (7 h vs 2.5 h, Figure 3). TNNT3 was found to be degraded by proteasome (Figure S2), because of the MG132 proteasome inhibitor doubled the half-life of TNNT3 and the TNNT3-p.R63C variant, but it could not change the intrinsic difference of their protein stabilities (Figure 4). TNNT3-p.R63C was found to be more stable than TNNT3, which was consistent with our previous hypothesis.

An important question is how p.R63C variant changed the protein stability of the TNNT3. We established a structural model of TNNT3 by PyMol and found that Arg63 is located on the helix as shown in the black square (Figure S3A). It was predicted that Arg63 could form hydrogen bond with Glu27-Asp28-Ile59-Gln60-Lys66-Asp67 of TNNT3 via molecular forces (Figure S3B). The substitution of Arg63 by cysteine disrupted hydrogen bond with Glu27-Asp28 and slightly reduce the stability of the TNNT3-p.R63C variant. But the whole protein structure was not changed (Figure S3C). The most difference between arginine and cysteine residue is their side chain. Based on our results and several previous studies,²⁸⁻³² we speculate that the p.R63C variant might increase TNNT3 protein stability and nuclear distribution by post-translational modification. Consistent with this possibility, phosphorylation and restricted proteolysis had been identified in TNNTs.²⁸ Several studies have reported that methylation of an arginine residue or S-nitrosylation (SNO) of a cysteine residue in some proteins might regulate cellular localization of the target protein and affect its degradation by the proteasome.^{29,30,32} Similar modifications could also occur in TNNT3 and other proteins. The p.W792R mutation in cardiac MYBPC leads to destabilization resulting in rapid degradation of itself,³¹ which further supports our hypothesis. R63 of wild-type TNNT3 might therefore be a potential site for methylation or other modifications. As previously reported, this possible modification could change its cellular distribution and promote degradation.³² The nonclassical nuclear localization mode of TNNT3 (Figure 5) and its proteasomal degradation pathway (Figures S1 and 4) found in this study are therefore consistent with our hypothesis. When R63 of TNNT3 was substituted by a cysteine, the cysteine residue became a novel potential site for SNO by endogenous nitric oxide (NO).³³ SNO at cysteine might prevent ubiquitination of the target protein and promote its stability.^{29,33,34} Additionally, SNO modification could change the conformation of the target protein and enhance its association with nuclear import proteins (such as importin, Ran) eventually promoting localization in the nucleus.^{30,33} These studies suggested that if the C63 of the TNNT3 variant was modified by NO, TNNT3-p.R63C could be also translocated into the nucleus, followed by conformation change and an increase in stability. Although the actual modification of the residue 63 is unknown at present, the possible roles of post-translational modification(s) in modulating TNNT3 stability and intracellular distribution should be further investigated.

An additional question involves how the p.R63C variant causes DA. TNNT3 could function as a transcriptional factor and share overlapping binding motifs with P53.²⁶ P53 is a well-known tumor suppressor protein and plays an important role in triggering apoptosis via multiple pathways. Previous evidences have suggested that P53 was critical for normal skeletal muscle function, including muscle differentiation and mitochondrial generation.³⁵⁻³⁸ Previous studies showed that overexpression of *TNNT3* led to apoptosis, while deletion of the DNA-binding leucine zipper domain or localization sequence significantly reduced its cytotoxicity.²⁵ We also found that the TNNT3-p.R63C variant accumulated in the skeletal muscle of affected subjects and speculated that the pathogenic role of the TNNT3-p.R63C variant was possibly associated with DA. An aberrant increase of nuclear TNNT3-p.R63C might upregulate TNNT3-dependent genes (such as *Cavβ1a*³⁹) and inhibit the transcription of P53-dependent genes (like *Bnip3L*³⁹). Competition between the TNNT3-p.R63C variant and P53 might disrupt the balance of gene regulation networks and cellular homeostasis, thereby resulting in apoptosis in muscle cells. Reducing the nuclear protein level of the TNNT3-p.R63C variant or blocking its transcription activity might therefore be used to treat DA patients.

At present, *TNNT3* variants usually cause muscle diseases.^{2,9,11,12,40} Because troponin C and troponin I are ubiquitously expressed in different types of cancer cells,²³ it is reasonable to speculate that *TNNT3* might be involved in tumor genesis or tumor metastasis by interfering with the tumor suppressive effect of P53. Notably, troponin T has been identified as a new marker on the surface of cultured tumor endothelial cells.⁴¹

In conclusion, our study showed that the p.R63C variant increased TNNT3 protein stability and promoted its nuclear accumulation. The p.R63C variant caused the abnormal degradation of TNNT3 and was assumed to be a transcriptional factor, whose mutation might play an important role in the genesis of DA. There is currently no drug that can effectively treat DA; however, our results implied that enhancing proteasome activity to degrade TNNT3 or blocking its transcription activity in the nucleus might effectively treat DA caused by the TNNT3-p.R63C variant. The results of this study therefore present the basis of development of a treatment for DA and provide a better characterization of patients with skeletal myopathies.

ACKNOWLEDGEMENTS

We thank all the patients and their family members for their participation in this project. And we are also grateful to all the organizations that funded this research: Medical Scientific Projects from Health Bureau of Zhejiang Province (2019RC275), Wenzhou Scientific Bureau (Y20170020), start-up funding (QTJ19019) from Wenzhou Medical University, Zhejiang Provincial Natural Science Foundation of China (No. Q16H200001), and National Key Research and Development Plan of China (2018YFC1002702).

CONFLICTS OF INTEREST

The authors declare no conflict of interest.

AUTHOR CONTRIBUTIONS

All authors conceived the study. Lu JF and Zhang H designed the research and wrote the manuscript; Lu JF, Li HZ, Zhang H, Hu L, and Luan ZT performed the experiments; Lu JF, Li HZ, Zhang H, Lin ZX, and Xu CY analyzed the data; Xu XQ and Tang SH performed the genetic counseling. Tang SH and Lou YL provided funding and edited the manuscript. All authors have read and approved the final manuscript. We thank International Science Editing (<http://www.internationalscienceediting.com>) for editing this manuscript.

DATA AVAILABILITY STATEMENT

The data presented in this study are available from the corresponding author on request.

ORCID

Shaohua Tang  <https://orcid.org/0000-0002-2918-8532>

REFERENCES

- Bamshad M, Van Heest AE, Pleasure D. Arthrogryposis: a review and update. *J Bone Joint Surg Am*. 2009;91(Suppl 4):40-46.
- Beck AE, McMillin MJ, Gildersleeve HIS, et al. Spectrum of mutations that cause distal arthrogryposis types 1 and 2B. *Am J Med Genet A*. 2013;161(3):550-555.
- Desai D, Stiene D, Song T, Sadayappan S. Distal arthrogryposis and lethal congenital contracture syndrome – an overview. *Front Physiol*. 2020;11:689.
- Jin JY, Wu PF, Fan LL, Yu F, Xiang R. A mutation of beta-tropomyosin gene in a Chinese family with distal arthrogryposis type I. *Int J Clin Exp Pathol*. 2017;10(11):11137-11142.
- Janelle G, Aikaterini KK. *MYBPC1*, an emerging myopathic gene: what we know and what we need to learn. *Front Physiol*. 2016;7:410.
- Xu Y, Kang QL, Zhang ZL. A *MYH3* mutation identified for the first time in a Chinese family with Sheldon-Hall syndrome (DA2B). *Neuromuscul Disord*. 2018;28(5):456-462.
- Whittle J, Antunes L, Harris M, et al. *MYH3*-associated distal arthrogryposis zebrafish model is normalized with para-aminobenzidine. *EMBO Mol Med*. 2020;12(11):e12356.
- Bo W, Zheng Z, Wang Z, Zhang X, Fu Q. A novel missense mutation of *TNNI2* in a Chinese family cause distal arthrogryposis type 1. *Am J Med Genet A*. 2016;170A(1):135-141.
- Sung SS, Brassington A-ME, Krakowiak PA, Carey JC, Jorde LB, Bamshad M. Mutations in *TNNT3* cause multiple congenital contractures: a second locus for distal arthrogryposis type 2B. *Am J Hum Genet*. 2003;73(1):212-214.
- Robinson P, Lipscomb S, Preston LC, et al. Mutations in fast skeletal troponin I, troponin T, and beta-tropomyosin that cause distal arthrogryposis all increase contractile function. *FASEB J*. 2007;21(3):896-905.
- Zhao N, Jiang M, Han W, et al. A novel mutation in *TNNT3* associated with Sheldon-Hall syndrome in a Chinese family with vertical talus. *Eur J Med Genet*. 2011;54(3):351-353.
- Daly SB, Shah H, O'Sullivan J, et al. Exome sequencing identifies a dominant *TNNT3* mutation in a large family with distal arthrogryposis. *Mol Syndromol*. 2014;5(5):218-228.
- Pehlivan D, Bayram Y, Gunes N, et al. The genomics of arthrogryposis, a complex trait: candidate genes and further evidence for oligogenic inheritance. *Am J Human Genetics*. 2019;105(1):132-150.
- Gordon AM, Homsher E, Regnier M. Regulation of contraction in striated muscle. *Physiol Rev*. 2000;80(2):853-924.
- Cao T, Thongam U, Jin JP. Invertebrate troponin: insights into the evolution and regulation of striated muscle contraction. *Arch Biochem Biophys*. 2019;666:40-45.
- Biesiadecki BJ, Chong SM, Nosek TM, Jin JP. Troponin T core structure and the regulatory NH2-terminal variable region. *Biochemistry*. 2007;46(5):1368-1379.
- Wei B, Jin JP. *TNNT1*, *TNNT2*, and *TNNT3*: isoform genes, regulation, and structure-function relationships. *Gene*. 2016;582(1):1-13.
- Fox MD, Carson VJ, Feng H-Z, et al. *TNNT1* nemaline myopathy: natural history and therapeutic frontier. *Hum Mol Genet*. 2018;27(18):3272-3282.
- Oki K, Wei B, Feng HZ, Jin JP. The loss of slow skeletal muscle isoform of troponin T in spindle intrafusal fibres explains the pathophysiology of Amish nemaline myopathy. *J Physiol*. 2019;597(15):3999-4012.
- Sandaradura SA, Bournazos A, Mallawaarachchi A, et al. Nemaline myopathy and distal arthrogryposis associated with an autosomal recessive *TNNT3* splice variant. *Hu Mutat*. 2018;39(3):383-388.
- Calame DG, Fatih J, Herman I, et al. Biallelic pathogenic variants in *TNNT3* associated with congenital myopathy. *Neurol Genet*. 2021;7(3):e589.
- Chase PB, Szczypinski MP, Soto EP. Nuclear tropomyosin and troponin in striated muscle: new roles in a new locale? *J Muscle Res Cell Motil*. 2013;34(3-4):275-284.
- Johnston JR, Chase PB, Pinto JR. Troponin through the looking-glass: emerging roles beyond regulation of striated muscle contraction. *Oncotarget*. 2018;9(1):1461-1482.
- Zhang T, Birbrair A, Wang ZM, Taylor J, Messi ML, Delbono O. Troponin T nuclear localization and its role in aging skeletal muscle. *Age*. 2013;35(2):353-370.
- Zhang T, Birbrair A, Delbono O. Nonmyofibrillar-associated troponin T3 nuclear and nucleolar localization sequence and leucine zipper domain mediate muscle cell apoptosis. *Cytoskeleton*. 2013;70(3):134-147.
- Lopez YON, Messi ML, Pratley RE, Zhang T, Delbono O. Troponin T3 associates with DNA consensus sequence that overlaps with p53 binding motifs. *Exp Gerontol*. 2018;108:35-40.
- Zhang H, Lu J, Wu S. Sp4 controls constitutive expression of neuronal serine racemase and NF-E2-related factor-2 mediates its induction by valproic acid. *Biochim Biophys Acta Gene Regul Mech*. 2020;1863(9):194597.
- Wei B, Jin JP. Troponin T isoforms and posttranscriptional modifications: evolution, regulation and function. *Arch Biochem Biophys*. 2011;505(2):144-154.
- Azad N, Vallyathan V, Wang L, et al. S-nitrosylation of Bcl-2 inhibits its ubiquitin-proteasomal degradation. A novel anti-apoptotic mechanism that suppresses apoptosis. *J Biol Chem*. 2006;281(45):34124-34134.
- Malik M, Shukla A, Amin P, et al. S-nitrosylation regulates nuclear translocation of chloride intracellular channel protein CLIC4. *J Biol Chem*. 2010;285(31):23818-23828.
- Smelter DF, de Lange WJ, Cai W, Ge Y, Ralphe JC. The HCM-linked W792R mutation in cardiac myosin-binding protein C reduces C6 FnIII domain stability. *Am J Physiol Heart Circ Physiol*. 2018;314(6):1179-1191.
- Piccolo LL, Mochizuki H, Nagai Y. The lncRNA hsr ω regulates arginine dimethylation of FUS to cause its proteasomal degradation in *Drosophila*. *J Cell Sci*. 2019;132:236836.
- Hess DT, Stamler JS. Regulation by S-nitrosylation of protein post-translational modification. *J Biol Chem*. 2012;287(7):4411-4418.
- Kohr MJ, Evangelista AM, Ferlito M, Steenbergen C, Murphy E. S-nitrosylation of TRIM72 at cysteine 144 is critical for protection against oxidation-induced protein degradation and cell death. *J Mol Cell Cardiol*. 2014;69:67-74.

35. Tamir Y, Bengal E. P53 protein is activated during muscle differentiation and participates with MyoD in the transcription of muscle creatine kinase gene. *Oncogene*. 1998;17(3):347-356.
36. Bartlett JD, Close GL, Drust B, Morton JP. The emerging role of p53 in exercise metabolism. *Sports Med*. 2014;44(3):303-309.
37. Yang ZJP, Broz DK, Noderer WL, et al. p53 suppresses muscle differentiation at the myogenin step in response to genotoxic stress. *Cell Death Differ*. 2015;22(4):560-573.
38. Saleem A, Carter HN, Iqbal S, Hood DA. Role of p53 within the regulatory network controlling muscle mitochondrial biogenesis. *Exerc Sport Sci Rev*. 2011;39(4):199-205.
39. Zhang T, Taylor J, Jiang Y, et al. Troponin T3 regulates nuclear localization of the calcium channel Cav β 1a subunit in skeletal muscle. *Exp Cell Res*. 2015;336(2):276-286.
40. Ju Y, Li J, Xie C, et al. Troponin T3 expression in skeletal and smooth muscle is required for growth and postnatal survival: characterization of *Tnnt3(tm2a(KOMP)Wtsi)* mice. *Genesis*. 2013;51(9):667-675.
41. Ara MN, Hyodo M, Ohga N, et al. Identification and expression of troponin T, a new marker on the surface of cultured tumor endothelial cells by aptamer ligand. *Cancer Med*. 2014;3(4):825-834.

SUPPORTING INFORMATION

Additional supporting information may be found in the online version of the article at the publisher's website.

How to cite this article: Lu J, Li H, Zhang H, et al. The distal arthrogryposis-linked p.R63C variant promotes the stability and nuclear accumulation of TNNT3. *J Clin Lab Anal*. 2021;35:e24089. <https://doi.org/10.1002/jcla.24089>